Effects of the thermal capacitance on the daily thermal performance of a CPC: An experimental investigation

Cite as: AIP Conference Proceedings **2191**, 020036 (2019); https://doi.org/10.1063/1.5138769
Published Online: 17 December 2019

G. Casano and S. Piva

Effects of the Thermal Capacitance on the Daily Thermal Performance of a CPC: an Experimental Investigation

G. Casano[1] and S. Piva[1, a)]

[1] DE Department of Engineering, Università di Ferrara, Via Saragat n.1, 44122 Ferrara, Italy

[a)]Corresponding author: pvs@unife.it

Abstract. The availability of reliable models for the prediction of the daily thermal behaviour of thermal solar collectors is of great relevance for a correct design of solar thermal systems. The most significant design parameters of a solar collector are outlet temperature and useful energy collection, both calculated on the base of the efficiency. The last, in turn, is commonly available on the base of experimental correlations obtained with the Steady State Testing method proposed by EN 12975-2. In these steady state tests, through the respect of very strict requirements, the contributions due to the thermal inertia of the solar collector becomes negligible. However, in its daily behaviour, it undergoes variable weather conditions with both regular and sharp changes of solar radiation. For these conditions the thermal inertia contributions become relevant in the correct prediction of its thermal behaviour. EN 12975-2 in Annex K suggests a modified equation for the prediction of the useful energy collection, based on a modification of the efficiency equation. A term dependent on the time derivative of the mean inlet/outlet water temperature is added. In this paper we examine experimentally the role played by this term for a Compound Parabolic Concentrator solar thermal collector.

INTRODUCTION

Solar thermal collectors are worldwide available for RESs thermal applications, because they allow a cheap and easy conversion of solar radiation in thermal energy. Solar radiation (seasonal, monthly or daily more generally the weather) is characterized by a time dependent behaviour. In the modelling of a thermal system this feature cannot be neglected. This strongly time dependent behaviour makes that the thermal capacitance of solar thermal collectors plays a significant role in the thermal energy conversion.

In general, we can say that theoretical and experimental investigations of solar thermal collectors development and utilization are largely available in the literature (see for instance [1] for updated information on water solar collectors and [2] for air solar collectors). However, research papers focused on the role played by the thermal inertia of these widespread components are limited.

A complete and interesting review of the information on this latter topic is given by Soriga and Badescu [3].

In thermal applications, like domestic hot water production and space heating, the thermal system behaviour is modelled through a set of experimentally gathered parameters, characterizing the thermal collector. In particular, the instantaneous efficiency of the collector is the main parameter used to correlate sun radiation and thermal production. This parameter is experimentally evaluated as a function of sun radiation and mean water and air temperature difference. International Standards for the codification of the procedure (EN 12975-2 for Europe and ISO 9806 for the rest of the word) are available.

In [4] and [5] Casano *et al.* give the instantaneous efficiency, experimentally evaluated with a test apparatus designed to follow as far as possible the Standard EN 12975-2 [6], for a new CPC solar thermal collector. Efficiency is evaluated by following the Outdoor Steady State (OSS) method. When using this correlation for the prediction of a daily behaviour of the CPC, Casano *et al.* [5] find out that the predicted values are always higher than the experimental ones. Presumably, the main source of disagreement has to be addressed to the thermal capacitance of the concentrating collectors, certainly significant in a daily simulation and neglected by the basic approach of the OSS method.

74th ATI National Congress
AIP Conf. Proc. 2191, 020036-1–020036-10; https://doi.org/10.1063/1.5138769
Published by AIP Publishing. 978-0-7354-1938-4/$30.00

In the present paper we study the daily behaviour of our CPC by including in the correlation used for predictions of the thermal production also the thermal inertia of the solar collector. It is shown that the predictions, if compared with experimental data, ensure a considerably better agreement.

Nevertheless, thermal inertia is not enough to completely justify the disagreement observed in [4] and [5] and confirmed in the new data here presented. Further elements need to be considered.

CPC AND TEST EQUIPMENT

A general description of the test equipment designed to follow as far as possible the Standard EN 12975-2 [6], and originally developed for an utilization with flat plate and evacuated tube solar collectors, is given in [7]. A description of its utilization to experimentally investigate a CPC solar thermal collector is given in [5]. A detailed description of our CPC is given in [4]. Here just some elements are given.

A line diagram of the hydraulic circuit of the measuring equipment with the CPC solar collector is shown in **Figure 1**, where the symbols for piping are taken from the standards for P&ID. In the hydraulic circuit, pressure, temperature and flow rate are measured. In particular, temperature is measured immediately upstream and downstream of the CPC solar collector. The flowrate (and the related fluid temperature) is measured downstream of the system used to condition the water temperature at the inlet of the CPC solar collector. These measurements are used to calculate the useful power. The global sun radiation on the CPC is measured with an Eppley Precision Spectral Pyranometer (PSP), while its beam component is measured with an Eppley Normal Incidence Pyrheliometer (NIP) moved by a tracking system Model ST-1. The diffuse solar irradiance is calculated as the difference between global and beam solar irradiance. For data reduction, also the ambient air temperature is measured. The CPC was placed with the receiver in the direction E-W. At the latitude of the city where it is located (Ferrara 44.84° N), in order to be able to capture the sun radiation for a wide part of the year, the capturing plane of the CPC was tilted of 30° with respect to the horizontal plane.

RESULTS AND DISCUSSION

In [5] Casano *et al*. compared some experimental data gathered in a typical spring day with the predicted thermal production based on the instantaneous efficiency, experimentally evaluated with the mentioned test apparatus, and given by:

$$\frac{Q_t}{A} = \eta_0 G - c_1 \left(T_{w,m} - T_a \right) \tag{1}$$

. The independent parameters of Eq. (1), η_0 and c_1, ($\eta_0 = 0.5882$ and $c_1 = 2.571$) were obtained by following the "Outdoor Steady-State" procedure of EN 12975-2 [6]. Steady state conditions and relatively short time intervals between data were guaranteed. It was evident that the predicted values were always higher than the experimental ones. The same comparison is here repeated for some different days. Note that hereinafter, the values of η_0 and c_1, will be considered known.

As the main source of disagreement we consider the thermal capacitance of the concentrating solar collector, presumably significant in daily data acquisitions, and neglected by the basic approach of the Outer Steady State method of EN 12975-2 [6]. The same Standard, in Annex K, suggests the introduction of further terms in Eq. (1), in particular of a term useful to consider the presence of an effective thermal capacitance of the collector. By following Annex K, Eq. (1) becomes:

$$\frac{Q_t}{A} = \eta_0 G - c_1 \left(T_{w,m} - T_a \right) - c_5 \frac{dT_{w,m}}{dt} \tag{2}$$

An analysis of the thermal capacitance of the CPC, constituted of a double pipe of glass, two copper pipes full of water and an aluminium fin for the thermal connection between pipes and glasses, gives:

$$\sum \frac{M_i}{A} c_{pi} = 6.54 \ \text{kJ/(m}^2\text{K)} \tag{3}$$

In the following we will use this value as the parameter c_5 in Eq. (2).

The first day under examination is a typical September day, characterized by a global solar irradiance typical of a fall day, with a clear sky and a negligible presence of clouds all along the day. The total irradiance was characterized

by a peak of 1000 W/m^2. The ratio between diffuse and global irradiance was constant and about 0.2.

In **Figure 2**, the measured thermal production, Q, the predicted thermal production obtained with Eq. (1), Q_t, and their difference, $Q-Q_t$, are shown. It is evident that for this day the predicted values are always higher than the experimental ones.

In **Figure 3** the difference between measured and predicted thermal production of the CPC is shown together with the time derivative of the mean inlet/outlet water temperature, as a function of time. The two parameters show the same average trend, even if for opposite signs (decreasing and positive values for the time derivative; decreasing, in absolute value, and negative values for the difference $Q - Q_t$). To this regular trend, a decidedly jagged contribution must be added, characterized by short period of evolution.

In **Figure 4** the new predicted thermal production of the CPC based on Eq. (2) is shown. A comparison of **Figures 2** and **4** shows a clearly better agreement of the data obtained with Eq. (2), with the experimental ones.

Nevertheless, a disagreement is still evident, greater in the morning and lower in the evening. The agreement improves clearly when adding a constant term to Eq. (2); this term is equal to 4.8 W/m^2.

In **Figure 5** the new thermal production is shown. When adding this constant term to Eq. (2), the predicted thermal production agrees very closely to the measured one. However, it is difficult to theoretically justify the constant term to be added to Eq. (2).

The second day under examination is still a typical September day; it is characterized by a global solar irradiance typical of a fall day, with clear sky and with the presence of scattered clouds around noon. The daily total solar irradiance shows a peak of 1000 W/m^2. The ratio between diffuse and global irradiance is about 0.3, smaller (0.2) in the morning and larger (0.4) in the afternoon.

For this second day, in **Figure 6** the measured thermal production, Q, the predicted thermal production, Q_t, and their difference $Q-Q_t$, are shown. It is evident that, as in **Figure 2**, the predicted values are always higher than the experimental ones. The difference is larger in the morning and smaller in the afternoon.

In **Figure 7** the difference between measured and predicted thermal productions of the CPC is shown together with the time derivative of the mean inlet/outlet water temperature, as a function of time. The two parameters show the same average trend, even if for opposite signs (decreasing and positive values for the time derivative; decreasing, in absolute value, and negative values for the difference $Q - Q_t$). To this regular trend, a decidedly jagged contribution must be added, characterized by short period of evolution. The fluctuations are definitely larger for the time derivative, unlike the difference of production.

For this second day, in **Figure 8** the new predicted thermal production of the CPC based on Eq. (2) is shown. This new production is obtained with the values of η_0 and c_1 obtained in [5], and with the parameter c_5 = 6.54 kJ/(m^{2}K) calculated with Eq. (3).

A comparison of **Figure 6** and **8** shows a clearly better agreement of the data obtained with Eq. (2) with the experimental ones. The production based on Eq. (2) is now equidistant from the experimental one; this means that the time behaviour (thermal capacitance) is now correctly considered. The two distributions show a quite constant distance, that can be eliminated by adding a constant term to the distribution based on Eq. (2). This term is now 18.4

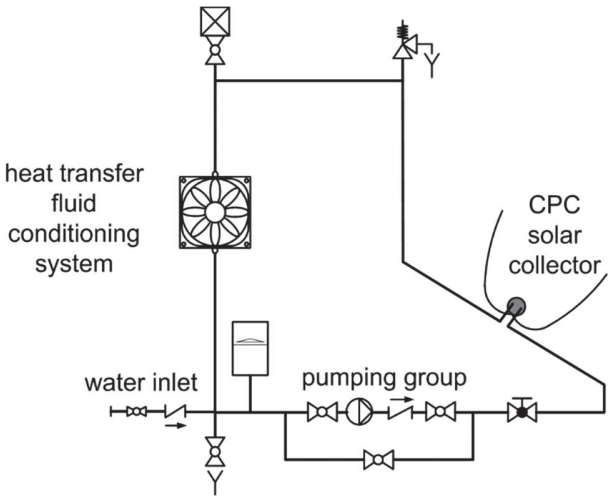

Figure 1. Scheme of the closed loop test equipment.

W/m^2, different from that necessary for the first day under examination.

In **Figure 9** the new thermal production is shown. When adding this constant term to Eq. (2), the predicted thermal production agrees very closely to the measured one. As for the results of the first day, it is difficult to theoretically justify the constant term to be added to Eq. (2). A further element characterizing the productions based on Eq. (2) is that around noon, when the weather becomes significantly cloudy, the predicted production shows a scattered behaviour that the experimental one does not show. This is due to the large scattering shown by the time derivative of the mean water temperature, which can be seen amplified in the thermal energy production.

Finally, we examine a typical day of March. This day is characterized by a global solar irradiance typical of a spring day, with a partly cloudy sky, especially in the morning. A peak of 1000 W/m^2 characterizes the total solar irradiance. The ratio between diffuse and global irradiance is about 0.30, increasing in the afternoon. For this third day, in **Figure 10** the measured thermal production, Q, the predicted thermal production, Q_t, and their difference, $Q-Q_t$, are shown. It is evident that, as in **Figure 2** and **6**, the predicted values are always higher than the experimental ones. The difference is larger in the morning and smaller in the afternoon. Furthermore, morning and afternoon are characterized by different trends: scattered thermal production due to clouds, in the morning; initially scattered and then quite regular production in the afternoon.

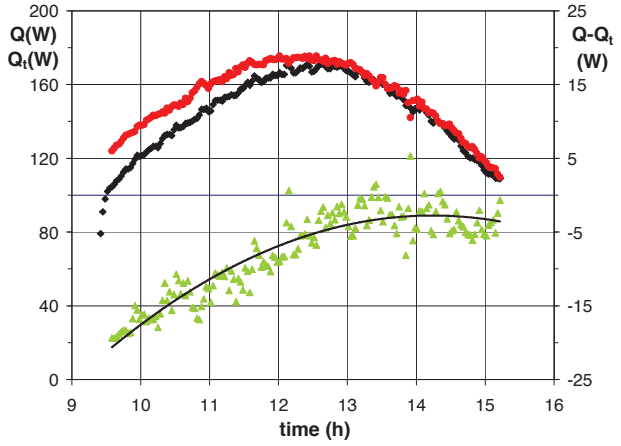

Figure 2. Measured (black points) and predicted (red points) thermal productions and their difference (green points).

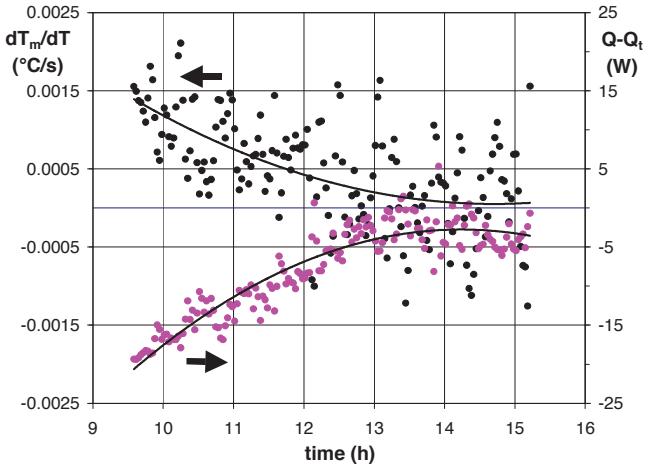

Figure 3. Difference between predicted and measured thermal productions (pink points) and time derivative of the mean water temperature (black points).

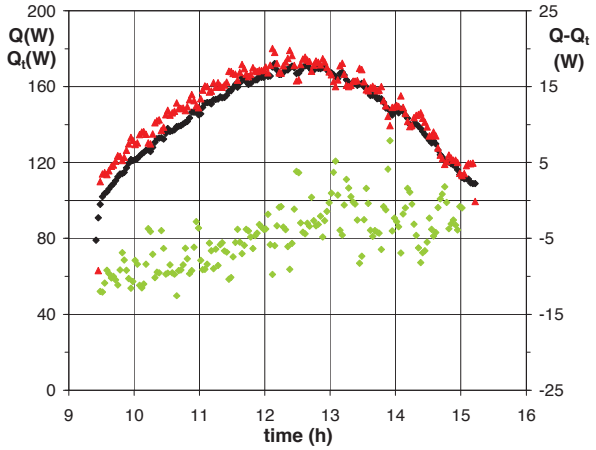

Figure 4. Measured (black points) and predicted (red points) thermal productions and their difference (green points).

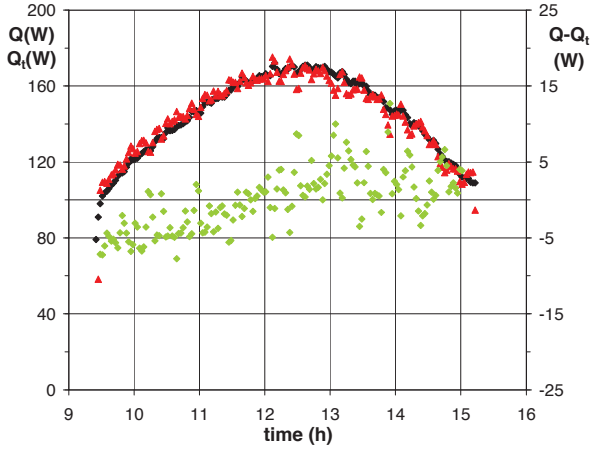

Figure 5. Measured (black points) and predicted (red points) thermal productions and their difference (green points).

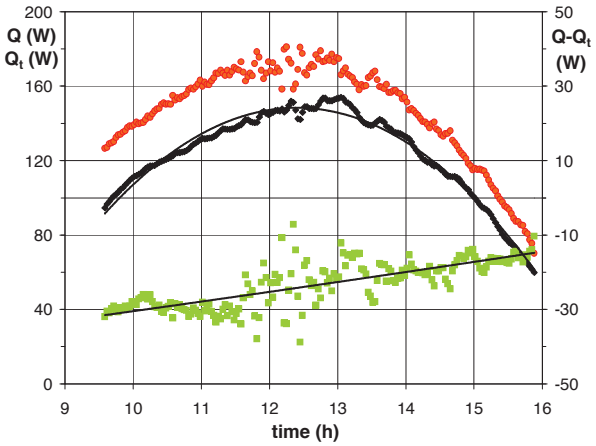

Figure 6. Measured (black points) and predicted (red points) thermal productions and their difference (green points).

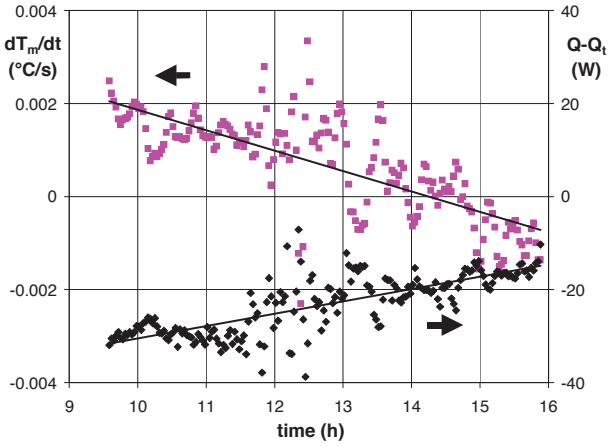

Figure 7. Difference between predicted and measured thermal productions (pink points) and time derivative of the mean water temperature (black points).

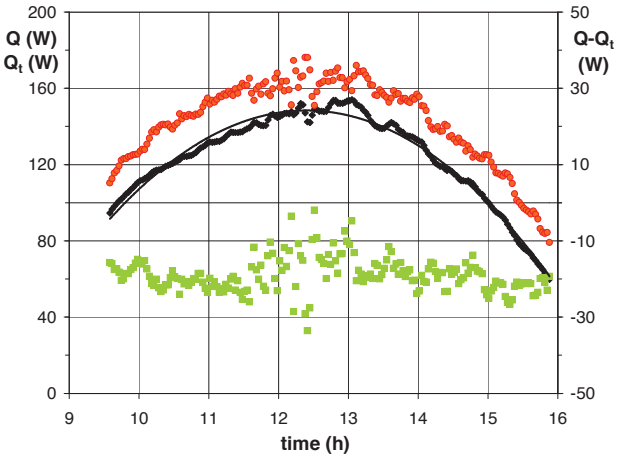

Figure 8. Measured (black points) and predicted (red points) thermal productions and their difference (green points).

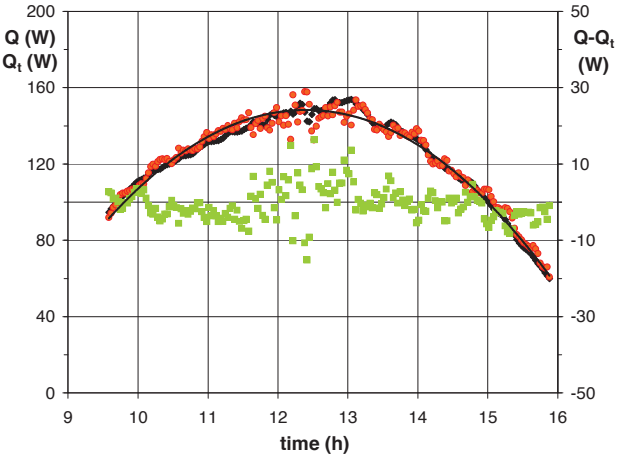

Figure 9. Measured (black points) and predicted (red points) thermal productions and their difference (green points).

This different behaviour is clearly evident in **Figure 11**, where the difference between measured and predicted thermal productions of the CPC is shown together with the time derivative of the mean inlet/outlet water temperature, as a function of time. In the afternoon the two parameters show the same average trend, even if for opposite signs (decreasing and positive values for the time derivative; decreasing in absolute value and negative values for the difference $Q - Q_t$). In the morning, the time derivative of the mean water temperature is so fluctuating, that it is difficult to recognize an evident trend.

For this third day, in **Figure 12** the new predicted thermal production of the CPC based on Eq. (2) is shown. This production is obtained with the values of η_0 and c_1 obtained in [5], and with the parameter $c_5 = 6.54$ kJ/(m^{2}K).

In **Figure 13** it is also evident that in the morning, characterized by a large and fast variation of the time derivative of the mean inlet/outlet water temperature, a very large fluctuation of the thermal production occurs, which is not so evident in the experimental data. The variation of the global irradiance is due to its direct component. This behaviour can be justified by considering that the characteristic time of the CPC is of the same order of magnitude of the weather fluctuations; then, the fast fluctuations due to the clouds cannot be "filtered" by the thermal inertia of the CPC.

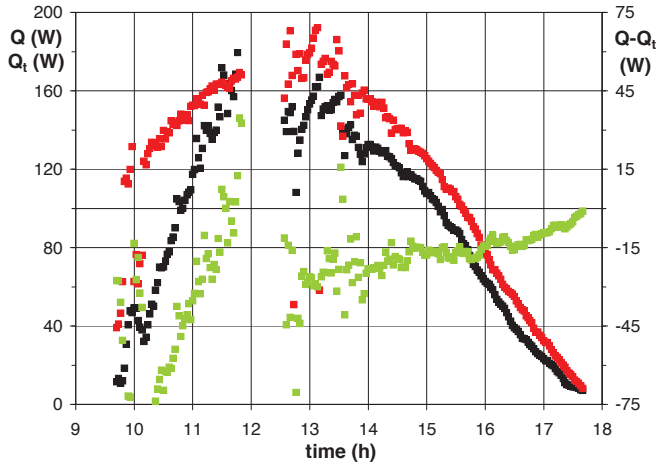

Figure 10. Measured (black points) and predicted (red points) thermal productions and their difference (green points).

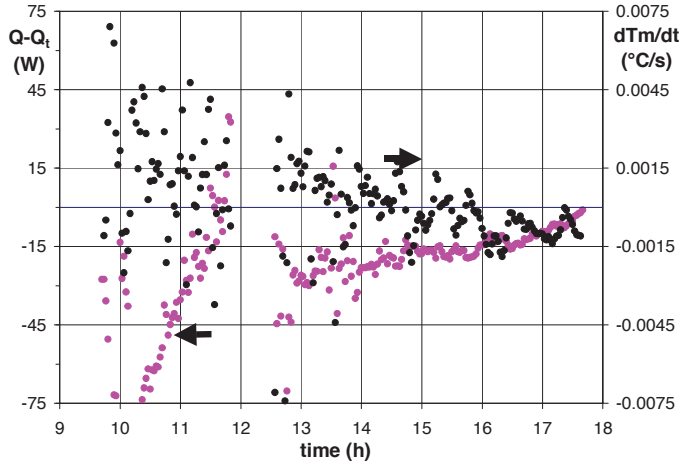

Figure 11. Difference between predicted and measured thermal productions (pink points) and time derivative of the mean water temperature (black points).

For this third day some further data are given. In **Figure 14**, total, direct and diffuse solar irradiations on the CPC are shown, together with the ratios direct / total and diffuse / total of the solar irradiation components. The ratio between diffuse and total solar irradiance is larger than the previous two cases. Significant fluctuations of the solar radiation are evident, in particular in the morning and in the first hours of the afternoon. The fluctuations are particularly large around noon. It is also evident that the characteristic time of these sun fluctuations is shorter than the data acquisition time (120 s). Since the characteristic time of the evacuated tube of the CPC solar collector (50-150 s, depending on the mass flow rate) is comparable to 120 s, the caption system is able to follow the weather fluctuation, as we can see in **Figure 15**.

In **Figure 15**, inlet-, outlet- and mean-water temperature and ambient temperature are shown, together with the difference between mean water temperature and ambient temperature. Just as for the sun radiation, significant fluctuations are also evident for the water and the ambient temperature. In particular, the difference between mean water and air temperature shows large and fast variations, necessarily reflected in the thermal production of the CPC. Significant fluctuations of the mean water temperature are the reason of large fluctuations of its time derivative (**Figure 11**); in the thermal production given by Eq. (2), the thermal capacity of the system is unable to dampen them.

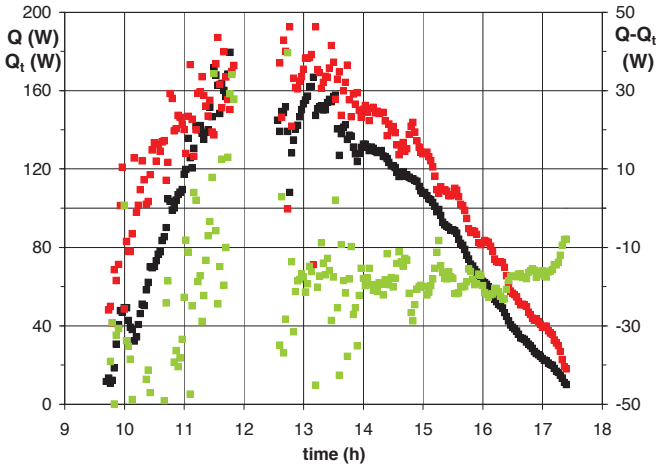

Figure 12. Measured (black points) and predicted (red points) thermal productions and their difference (green points).

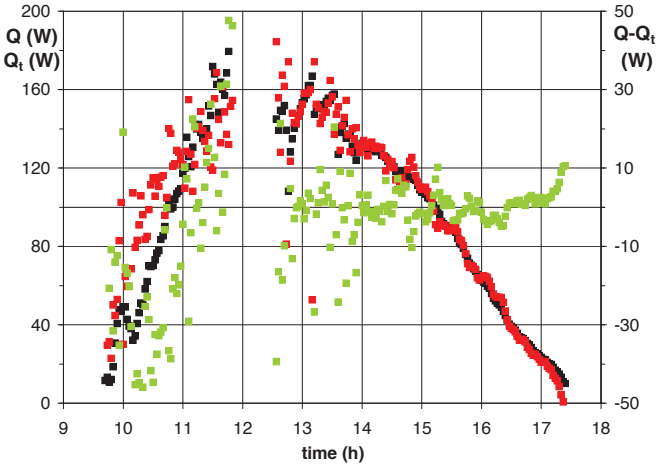

Figure 13. Measured (black points) and predicted (red points) thermal productions and their difference (green points).

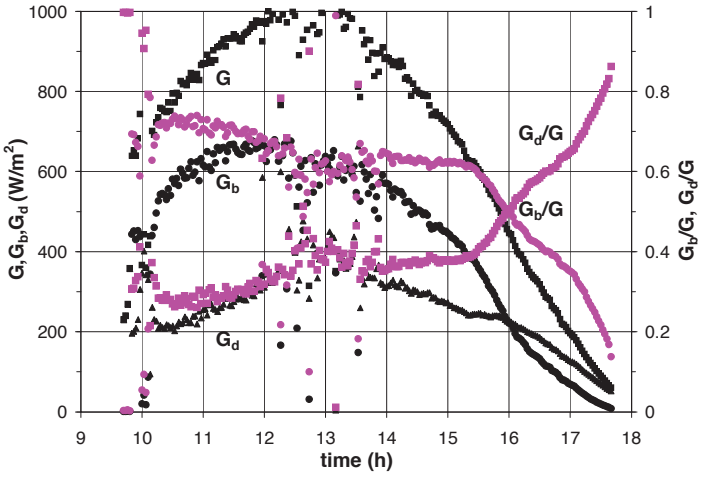

Figure 14. Total, direct and diffuse solar irradiation on the CPC (black points) and ratio between direct / diffuse component and total solar irradiation (pink points).

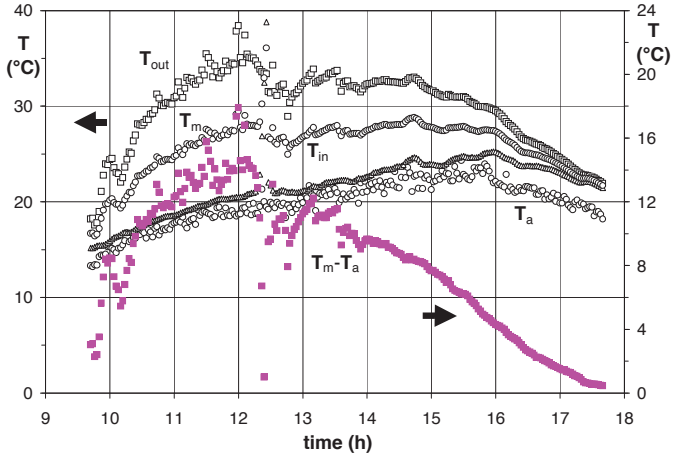

Figure 15. In, out, mean water temperature and ambient temperature (white points) and difference between mean water and ambient temperature (pink points).

CONCLUDING REMARKS

In a previous paper [5] we supposed that the thermal inertia was responsible of the disagreements between experimental data of thermal production of a CPC solar collector and predictions based on the efficiency of the collector measured in steady state conditions (Equation (1), taken from the Standard EN 12975-2 [6]).

For three days, characterized by different levels of cloudiness, it is shown that the effect of the thermal inertia of the CPC solar collector exists and is significant. This effect becomes evident in two ways:

- the predicted production is always higher than the experimental one; it means that in the applications part of the solar energy captured by the collector is used to satisfy the request of the inertial component that is not considered by the "steady state" efficiency;
- the predicted production, when compared to the experimental one, seems to be rotated clockwise around the sunset; it means that the inertial effect is significant in the morning and negligible in the afternoon.

The equation for a "steady state" efficiency can be modified, by considering a thermal inertia term, as suggested by the Standard EN 12975-2 [6], here considered in Equation (2). As the value of the new parameter introduced in

the latter equation, the theoretical value of the thermal capacitance per unit of area of the CPC collector is used.

With this "unsteady state" efficiency the predicted thermal productions seem to be in agreement with the measurements. The clockwise rotation really disappears and the difference between the two different productions can be taken in to account with a further constant parameter.

However, this constant parameter, different day-to-day, at the moment cannot be theoretically justified; it seems to be related to ratio between diffuse and direct solar radiation, and to the presence of cloudiness.

Furthermore, the predictions based on the "unsteady state" efficiency (Equation (2) from the Standard EN 12975-2 [6]) are unable to follow the measurements in the cloudy days. In these days the characteristic times of the weather phenomena are evidently shorter than the characteristic time of the CPC solar collector, mainly related to its thermal inertia and to the flow conditions. In these cloudy days the average behaviour of the CPC solar collector is satisfactorily predicted, while for the fast variations due to the clouds, and more generally to the weather, the predictions are unsatisfactorily.

The research will continue in these two directions:

- how to separately consider in the assessment of efficiency, direct and diffuse components of the solar radiation;
- how to separate the average behavior of the CPC solar collector from that produced by the fast variations due to clouds, and more generally due to the weather.

REFERENCES

1. S. A. Kalogirou, Progress in Energy and Combustion Science **30** (3), 231-295 (2004).
2. Y. Tian, C. Zhao, Applied Energy **104**, 538–553 (2013).
3. I.. Soriga, V. Badescu, Energy Conversion and Management **111**, 27-37 (2016).
4. G. Casano, M. Fossa, S. Piva, Int. J. Heat and Technology **35**, S.I. 1, S179-S185 (2017).
5. G. Casano, M. Fossa, S. Piva, Int. J. Heat and Technology **35**, 4, 827-835 (2017).
6. EN 12975-2. *Thermal solar systems and components - Solar collectors - Part 2: Test methods* (2006).
7. G. Casano, S. Piva, Int. J. Heat and Technology **31**, 25-30 (2013).

NOMENCLATURE

A	CPC aperture surface, m^2
G	global solar irradiance, Wm^{-2}
G_b	direct solar irradiance, Wm^{-2}
G_d	diffuse solar irradiance, Wm^{-2}
G	global solar irradiance, $W\ m^{-2}$
Q	useful power extracted from collector, W
t	time, h
T	temperature, °C or K
T*	reduced temperature difference, Eq. (7)

Greek symbols

η	collector efficiency, Eq. (6)

Subscripts

0	zero loss
a	ambient
b	direct
d	diffuse
in	inlet
m	in/out mean
out	outlet
t	predicted
w	water